

Trends of air pollution over the East China Sea analyzed with 20 years aerial observation data

HATAKEYAMA, Shiro^{1*}, IKEDA, Keisuke¹, TAKAMI, Akinori², MURANO, Kentaro³, BANDOW, Hiroshi⁴

¹Tokyo University of Agriculture and Technology, ²National Institute for Environmental Studies, ³Hosei University, ⁴Osaka Prefecture University

[Introduction] We have continued aerial observations over the seas between Asian continent and Japan for twenty years in order to analyze the transport and transformation of log-range transported atmospheric pollutants. Covered areas are the East China Sea, the Sea of Japan, and the Yellow Sea. During this period the economic growth in East Asia, particularly in China, was remarkable and as a result emission of atmospheric pollutants increased tremendously. In this report we will show the results of our analyses on the long term trend of gaseous pollutants such as SO₂ and ozone as well as ionic components of aerosols.

[Used data] The data used for the analyses were 11 data sets, i.e., those obtained in PEACAMPOT program in October, 1991, November, 1992, March and December, 1994, January and December, 1997, February, 1999, and March 2001 as well as those in LEXTRA program in March-April, 2008, and those in ASEPH project in October, 2009 and December, 2010.

Aircrafts employed were Cessna 404, and Fairchild Swearingen chartered from Showa Aviation Company, and Beachcraft Kingair 200T chartered from Diamond Air Service. The target of the observations was lower tropospheric (below 3000 m) atmosphere.

Items of observations common for 20 years experiments were gaseous species such as ozone, SO₂, and NO_x (NO_y) as well as ionic species in aerosols collected with a high-volume tape sampler. Sulfate, nitrate, ammonium, and calcium were the main ionic species analyzed.

[Results and Discussion] Anthropogenic species in the gas phase (SO₂ and ozone) and aerosol phase (SO₄²⁻, NO₃⁻, and NH₄⁺) were analyzed in this presentation.

Sulfate and ammonium showed a quite similar trend. That means sulfate and ammonium existed in the form of (NH₄)₂SO₄ and/or NH₄HSO₄. It seems that sulfate is decreasing from 2001. Unfortunately, since the data between 2002 and 2007 are lacking (we carried out aerial observations over the main land China in that period), it is not obvious. However, it is reported that the emission of SO₂ in China is decreasing from 2006 (Lu et al., 2010). Our results seem in accordance with the report, although decreasing trend of SO₂ was not very clear in this work.

In contrast, was low before December, 1997 (maximum 1.5 ug/m³), but it is increasing after 1999 having maximum concentrations exceeding 7 ug/m³. It seems to show an increasing trend. Emission of NO_x, which is a precursor of NO₃⁻, is increasing in China (Ohara et al., 2007), and that can cause increase of NO₃⁻ over the East China Sea. More clearly, the ratio of NO₃⁻/SO₄²⁻ increases reflecting the trends of sulfate and nitrate.

Ozone was analyzed using histograms for former period (1991-1999) and latter period (2001-2010). In 1990s ozone in the range of 40<O₃ conc.<45ppb appeared most frequently, whereas ozone in the range of 65<O₃ conc.<70ppb appeared most frequently in 2000s. This feature was more remarkable in the lower troposphere below 1500 m. Ozone in the boundary layer is increasing because of anthropogenic emission of NO_x in China.

Lu, Z., et al., (2010). *Atmospheric Chemistry and Physics*, 10(13), 6311-6331. doi:10.5194/acp-10-6311-2010.

Ohara, T., et al., (2007). *Atmospheric Chemistry and Physics Discussions*, 7(3), 6843-6902. doi:10.5194/acpd-7-6843-2007.

Keywords: aerial observation, East China Sea, aerosol, ionic species, trans-boundary air pollution, ozone

Chemical analysis of transported and urban aerosols

MIYOSHI, Takao^{1*}, TAKAMI, Akinori¹, IREI, SATOSHI¹, SATO, Kei¹, SHIMONO, Akio², HIKIDA, Toshihide², HARA, Keiichiro³, HAYASHI, Masahiko³, KANEYASU, Naoki⁴, HATAKEYAMA, Shiro⁵

¹NIES, ²SLS, ³Fukuoka U, ⁴AIST, ⁵TUAT

East Asia is a source of large amounts of anthropogenic SO₂, NO_x, and volatile organic compounds in the atmosphere. The region's economy is developing rapidly, and energy consumption is also increasing. There is serious concern that the emissions of atmospheric pollutants will increase accordingly. Fukuoka City is located in the northern Kyushu and is influenced by anthropogenic pollutants transported from the continent. On the other hand, Fukuoka City is a large city, which has a population of 1.5 million and is a source of large amounts of anthropogenic pollutants. It is thought that there are pollutants from the local area and the continent in Fukuoka City in spring. We measured chemical components and mass concentrations of atmospheric aerosols at Fukuoka University and analyzed the data by Positive Matrix Factorization (PMF) method in order to research the influence of trans-boundary air pollution on air quality of urban areas.

Chemical components of atmospheric aerosols were measured by Aerosol Mass Spectrometer (Q-AMS) at the fourth floor of Building 18 (Faculty of Science), Fukuoka University. The chemical components were sulfate, nitrate, ammonium, chloride and organics. Mass concentration of PM_{2.5} was observed by TEOM (RP1400) at the roof of Building 18.

The observation showed periods in which sulfate was rich and in which nitrate and organics were rich. The previous measurement by Q-AMS at Fukue Island, Nagasaki and Cape Hedo, Okinawa implied sulfate-rich period was influenced by long-range transport from the continent and nitrate and organics-rich period was influenced by atmospheric pollutants from Japan and Korea.

In sulfate-rich period, the size distribution had one mode of around 0.6micrometer and was similar to the results at Fukue Island and Cape Hedo. Analysis by back trajectory (NOAA-HYSPLIT4) showed the air mass was transported from China. In nitrate and organics-rich period, the size distribution had two modes of around 0.2 and 0.6micrometer. In the cases where air quality was influenced by pollutants from only urban areas, a single mode was around 0.1micrometer. Sulfate, nitrate and organics showed bi-modal distribution characteristically and nitrate was rich in a mode of smaller size in this measurement. These results suggested air quality in Fukuoka City was not mainly influenced by long-range transport. However because sulfate concentration was relatively high and the m/z=44 signal corresponding to COO fragment in the mass spectra was observed, the pollutants both from the continent (long-range transport) and from domestic sources and Korea (middle-range transport: at most 100-200km) were transported to Fukuoka City.

Organics were analyzed using PMF method. As a result the factors corresponding to aerosols from urban areas and the continent were obtained. The contribution of each factor was also estimated.

Keywords: Fine Particle, Fukuoka, Q-AMS, PMF

Estimating health effects of atmospheric aerosol particles

UEDA, Kayo^{1*}, NITTA Hiroshi¹

¹National Institute for Environmental Studies

There is evidence supporting that atmospheric aerosol particles inhaled into the respiratory tract have adverse health effects on respiratory and cardiovascular systems. Toxicological studies have shown the following biological mechanisms. Aerosol particles deposited on airway and alveolar surface could 1) induce inflammation in the lung and its airways which results in lung damage, 2) induce respiratory hypersensitivity and aggravate asthma and allergic rhinitis, 3) increase susceptibility to respiratory infection. It is also suggested the pathways for cardiovascular diseases. Particles could 1) trigger arrhythmias and cause adverse cardiac function by changing autonomic nervous system regulation, 2) increase superoxide and accelerate remodeling of blood vessels, 3) activate platelet/coagulation which trigger the atherothrombotic events of coronary arteries.

Most of the studies examining the association between ambient aerosol particles and human health using epidemiological methods are from North America and Europe. In those studies, the magnitude of the health effects of ambient aerosol particles is estimated by comparing the daily number of health events (such as death, hospitalization, and emergency room visits) and daily concentration of particles. In Japan, we combined the mortality data and concentration of PM_{2.5} (particles with diameter less than 2.5 micrometer) measured at the monitoring stations for 20 cities during 2002-2004, and observed that PM_{2.5} concentration was positively associated with the number of deaths due to respiratory diseases. Although the results did not show significant association between PM_{2.5} concentration and mortality due to cardiovascular diseases (heart diseases and stroke), we found that PM_{2.5} was associated with mortality specific cardiac disease (acute myocardial infarction).

Previous epidemiological studies have also suggested the health effect varies by area and season. It is possible that the difference in particles composition is attributed to the effect size.

Keywords: aerosol particles, health effects

Perspective on atmospheric chemistry and climate change from aerosols

TAKEMURA, Toshihiko^{1*}

¹RIAM, Kyushu University

Atmospheric aerosols, as well as causing respiratory and allergic diseases, submicron-sized material in order to circulate throughout the body are incorporated into the blood from the lungs, which is known to potentially cause any diseases. Japan had a problem of air pollution by aerosols throughout a period of high economic growth after World War II, and in recent years it has been frequent around the western region that air pollution caused by rapid economic growth in China (Yamaguchi and Takemura, 2011). As China has suffered severe air pollution remains (Washington Post, 2012), it is necessary to clarify the physical and chemical properties, behavior in the atmosphere, and health effects of aerosols. In particular, considering that the desulfurization equipment is gaining popularity even in developing countries, quantitative assessment and prediction of properties of nitrate particles, with complex chemical reaction than sulfate, and organic particles will become more important. As for the increased levels of photochemical oxidant which is one of the air pollution, in Japan, the advisory and warning are made known to the public when the level is high because the criteria of them is clear. On the other hand, the communication system to the public has not been established when the aerosol concentration is high with low concentrations of photochemical oxidant and Asian dust. With the Japan's environmental standard of PM_{2.5} set in 2009, it is important to quickly develop a system to disseminate information on observation and forecasting of air pollutants.

Aerosols, in addition to air pollution, absorb or scatter solar and infrared radiation (direct effect), and act as nuclei of clouds (indirect effect), so that the change in their concentration causes climate change by changing the energy balance in the atmosphere. In addition, the aerosol contribution to the marine ecosystem as a nutrient, changes in snow surface albedo due to deposition of the aerosols that absorb radiation, providing opportunities for chemical reactions (heterogeneous reactions), and etc., have been pointed out to impact on climate. However, the evaluation of the radiative forcing relative to the preindustrial era in the Fourth Assessment Report (AR4) of the Intergovernmental Panel on Climate Change (IPCC) still has a large uncertainty; -0.1 to -0.9 $W m^{-2}$ for the direct effect, -0.3 to -1.8 $W m^{-2}$ for the first indirect effect, and 0.0 to $+0.2$ $W m^{-2}$ for the change in snow surface albedo due to deposition of black carbon. There are various factors to produce these uncertainties both in observation and numerical modeling studies. As the aerosol radiative forcing, even though they are quantitatively similar to that of greenhouse gases, has large uncertainties, reduction of the uncertainties is a major key in terms of predicting future climate change.

In this lecture, the global aerosol climate model SPRINTARS (Takemura et al., 2005, 2009) provides central topics for researches in order to think about the direction in addressing the above issues.

References

Takemura, T., et al. (2005), *J. Geophys. Res.*, 110, doi:10.1029/2004JD005029.

Takemura, T., et al. (2009), *Atmos. Chem. Phys.*, 9, 3061-3073.

Washington Post (2012), http://www.washingtonpost.com/world/asia-pacific/beijing-makes-rare-concession-on-pollution-measure/2012/01/19/gIQApsI6BQ_story.html.

Yamaguchi, Y., and T. Takemura (2011), *Tenki*, 58, 965-968 (in Japanese).

Keywords: aerosol, climate change, atmospheric chemistry, atmospheric pollution

Underlying uncertainty in future projection of marine ecosystem feedbacks to climate change

ITO, Akinori^{1*}, KOK, Jasper F.², FENG, Yan³, PENNER, Joyce E.⁴

¹JAMSTEC, ²Cornell University, ³Argonne National Laboratories, ⁴University of Michigan

It is widely recognized that uncertainty in the deposition flux of bioavailable iron to the ocean is large and that the value assumed can influence the air-sea carbon dioxide fluxes and thus radiative forcing significantly. Global models have been used to deduce atmospheric iron supply to the ocean, but uncertainty in the deposition flux remains large, in part because of uncertainty in the size distribution of mineral aerosols. We used a global chemical transport model to investigate the effect of the estimated size distribution of dust on the bioavailable iron deposition. Simulations are performed with six different size distributions for dust aerosols at emission using similar aerosol optical depths (AODs) to constrain the total emission flux of dust. The global dust emission rate using a recent theoretical estimate for the dust size distribution at emission is about two times larger than the average of estimates using the other four empirical size distributions. In contrast to the large differences in total emissions, the dust emission of fine particles is relatively robust, due to the strong constraint of AOD on clay emission. Our model results indicate that soluble iron (SFe) deposition is relatively invariant to the dust size distribution at emission in significant portions of the open ocean, where fine particles play a dominant role in soluble iron supply. In contrast, the use of the theoretical size distribution suggests a larger deposition of SFe (by a factor of 1.2 to 5) in the South Atlantic. These results could have important implications for the future projection of marine ecosystem feedbacks to climate change and highlight the necessity to improve the dust size distribution.

Keywords: mineral aerosol, atmospheric chemical transport model, soluble iron supply, size distribution, air pollutant, climate change

Development and validation of a size and mixing state resolved three-dimensional model

MATSUI, Hitoshi^{1*}, KOIKE Makoto¹, KONDO Yutaka¹, MOTTEKI Nobuhiro¹

¹Graduate School of Science, University of Tokyo

The mixing state of black carbon (BC) aerosols is one of the most important issues for estimating radiative and climatic impact of aerosols. In this study, we developed a size and BC mixing state resolved three-dimensional model based on the WRF-chem model (MS-resolved WRF-chem). We adopted two-dimensional aerosol bin representation: one dimension is aerosol dry diameter (12 bins between 40 nm and 10 μ m) and another dimension is BC mass fraction to total aerosol mass concentrations in dry condition (10 bins). The detailed aerosol microphysical processes such as condensation/evaporation and coagulation are simulated with 120 aerosol bins.

The MS-resolved WRF-chem model was applied to East Asia in March and April 2009 when the A-FORCE aircraft campaign was conducted over the Yellow Sea and the East China Sea. Model calculations were compared with observed BC mixing state obtained by a single-particle soot photometer (SP2). Model calculations generally reproduced the main features of observed BC mixing state (e.g., BC-free to total aerosol number concentration ratio, diversity of shell (total particle dry diameter) to BC core diameter ratios (SC ratio), mean SC ratio, and their temporal variations and diameter dependence).

We evaluated the impact of microphysical processes (condensation and coagulation) on the BC mixing state of atmospheric particles. Sensitivity simulations suggest that BC aging processes can be classified into two regimes. Condensation processes are dominant for the growth of thinly coated BC particles (higher BC mass fractions), while coagulation processes are necessary to produce thickly coated BC particles (lower BC mass fractions). Although the impact of coagulation processes on total aerosol mass concentrations are very limited, they would be important in terms of the optical and radiative properties and the lifetime of BC.

We also conducted sensitivity simulations focused on mixing state of emissions. We compared two simulations: 1) the base case simulation in which all the BC emissions were assumed to be externally-mixed particles and 2) the sensitivity simulation in which about 50% of BC emissions were assumed to be internally-mixed particles based on the measurements at an urban site in Tokyo. The results suggest that the mixing state in emissions is an important factor to understand the BC mixing state of atmospheric particles more quantitatively.

Keywords: Aerosol, Black carbon, Mixing state, Regional three-dimensional model, Bin model, East Asia

Optical properties of secondary organic aerosols from photooxidation of toluene: wavelength and NO_x dependence

NAKAYAMA, Tomoki^{1*}, SATO, Kei², MATSUMI, Yutaka¹, IMAMURA, Takashi², YAMAZAKI, Akihiro³, UCHIYAMA, Akihiro³

¹Solar-Terrestrial Environment Laboratory, Nagoya University, ²National Institute for Environmental Studies, ³Meteorological Research Institute

Atmospheric aerosol plays an important role in visibility, health effects, heterogeneous chemistry, and radiation balance from local to global scale. Recently, it has been suggested that some organic aerosols, which is called 'brown carbon', can absorb solar radiation, especially at the ultraviolet (UV) and shorter visible wavelengths and contribute to the radiation balance and photochemical reactions in the atmosphere. Our group [Nakayama et al. JGR2010] retrieved the real and imaginary parts of RI at 355 and 532 nm for the SOAs generated from the photooxidation of toluene in the presence of NO_x (toluene-SOAs) under the condition of [HC]_{ini} = 4.0 ppmv and [NO_x]_{ini} = 540 ppbv, by measuring extinction and scattering coefficients using cavity ring-down spectrometer (CRDS) and nephelometer, respectively. Non-negligible *k* value was obtained at 355 nm, while no evidence of light absorption by the toluene-SOAs at 532 nm was found because of the difficulty to quantify the small difference between extinction and scattering coefficients. Therefore, direct measurement of absorption coefficient is desired for the accurate determinations of the small *k* value. Nitrated aromatics compounds such as nitro-cresols were considered as plausible sources of the light absorption at UV and shorter visible wavelength. The production quantum yield of nitrated aromatic compounds may depend on initial mixing ratio of [NO_x]_{ini}, however, the *k* values were measured under limited [NO_x]_{ini} conditions. In this work, wavelength and NO_x dependence of the complex RI values of the toluene-SOAs are investigated in detail. To determine small *k* value accurately, a three wavelength photoacoustic spectrometer (PASS-3) are applied to measure the light absorption of the SOAs suspended in air, directly.

The SOAs were generated in a 6 m³ Teflon coated stainless steel photochemical smog chamber in the absence of seed particles. The reaction mixture of toluene and NO was continuously irradiated by light from a xenon arc lamp through Pyrex filters after the addition of a small amount of methyl nitrite as a source of OH radicals. Four experimental runs were conducted for toluene-SOAs with different [NO_x]_{ini} conditions (109-571 ppb) to examine the NO_x dependence of RI values. When the mass concentration of the SOAs started to increase, the SOAs were introduced into the PASS-3 (absorption and scattering at 405, 532, 781 nm) and a custom-built CRDS instruments (extinction at 532 nm) to measure optical properties. Chemical properties of aerosols were also measured by an Aerodyne aerosol mass spectrometer (ToF-AMS) driven in V-mode. The size distributions of SOAs were measured by a scanning mobility particle sizer (SMPS).

Absorption, scattering, and extinction efficiencies of SOAs are calculated by dividing the absorption, scattering, and extinction coefficients by total mobility cross sections measured with the SMPS. Refractive index of the SOAs is determined by comparing the size parameter dependence of extinction, scattering, and absorption efficiencies with Mie theory. The significant *k* values at 405 nm, which are almost linearly increased from 1.8*10⁻³ to 7.2*10⁻³ with increasing of [NO_x]_{ini} from 107 to 571 ppbv, are obtained. At 532 nm, non-negligible *k* value (1.0*10⁻³) is also obtained under high [NO_x]_{ini} conditions, while the values for other runs are negligibly small within the experimental uncertainties. If the light absorbing species involving nitro-aromatic compounds are assumed to be mainly produced from the reaction of toluene-OH adduct with NO₂, the observed strong [NO_x]_{ini} dependence of the *k* values at 405 nm can be explained by the change in the formation yield of these species. In the presentation, relationship with chemical properties and the atmospheric implications of the results will also be discussed.

Keywords: Aerosol optical properties, Secondary organic aerosol, Brown carbon, Refractive index, Mass absorption cross section, Toluene

Optical properties of diesel exhaust particles

GUO, Xuesong^{1*}, NAKAYAMA, Tomoki¹, MATSUMI, Yutaka¹, Hiyroyuki Yamada², TONOKURA, Kenichi³, INOMATA, Satoshi⁴

¹Solar-Terrestrial Environment Laboratory, Nagoya University, ²National Traffic Safety and Environment Laboratory, ³The University of Tokyo, ⁴National Institute for Environmental Studies

Aerosol particles influence climate directly by scattering and absorbing of an incoming solar radiation and indirectly by acting as cloud condensation nuclei. Diesel exhausts particles (DEP) are known as one of main anthropogenic source of element carbon (EC), and organic carbon (OC). The light absorption of BC is generally considered to be increased by coating with OC, which is called lensing effect. In addition, recently light-absorbing OC, 'brown carbon', involving humic-like substance (HULIS), organonitrate, and nitro-aromatics etc., has been proposed as a source of significant absorption, particularly in the near-UV. However, contributions of lensing effect and brown carbon for DEP have not been well known because of the difficulty in the accurate measurement of light absorption of internally mixed BC particles without collecting on filter. In this study, a photoacoustic soot spectrometer three wavelength (PASS-3) has been applied to research optical properties of DEP.

A diesel engine was operated in a car driven on a chassis dynamometer with an urban driving mode (JE05) and constant speed mode (0 km/h or 70 km/h). The diesel exhaust was diluted and then sent through a heater before the measurement of optical properties. Absorption and scattering coefficients at 405, 532, and 781 nm of the DEP are measured by the PASS-3. Size distributions of DEP before and after heating are also measured by two scanning mobility particles sizers (SMPS) during constant mode experiments.

For the JE05 mode, optical properties were measured with inlet temperatures of 20, 100, and 300 degC. Enhancement of scattering coefficient was observed during acceleration and deceleration patterns before and after high speed driving (~80 km/h) at 25 and 100 degC. The result that the enhancement was not detected at 300 degC indicates that emission of volatile OC compositions increased during the patterns. From the observed absorption coefficients, absorption Angstrom exponent (AAE) is calculated. The AAE values between 405 and 532 nm are found to increase during the periods when volatile OC compositions increase at 20 and 100 degC, while the AAE values are almost constant at 300 degC. By assuming that OC was removed by heating up to 300 degC and that light absorption by OC is negligible at 781 nm, the contributions of light absorption by OC to total light absorption at 405 and 532 nm are estimated to be ~15% and <5%, respectively.

For the constant mode, optical properties of DEP were measured with variety of inlet temperatures between 20 and 400 degC. No significant temperature dependence of AAE between 405 and 532 nm was found in both case of idling and 70 km/h patterns. The result indicates that the contribution of light absorption by OC is small (<6%). By comparing absorption coefficients at 20 and 400 degC, increase in light absorption by coating during idling and 70 km/h patterns are estimated to be 20 and 15%, respectively.

Recently, Dr. Inomata and co-workers detected nitro-aromatics in gas and particle phases of diesel exhausts from the same car. The concentrations of nitro-aromatics in gas phase are significantly high during the same periods, when the light absorption by OC was found in the present study. Therefore, nitro-aromatics in DEP can be considered as plausible sources of light absorbing OC, observed in this study.

Keywords: Aerosol optical properties, Diesel exhaust particle, Photoacoustic spectroscopy, Lensing effect, Black carbon, Brown carbon

Direct measurement of aerosols and cloud residues using airborne CVI

MATSUKI, Atsushi^{1*}, SCHWARZENBOECK Alfons², QUENNEHEN Boris², DEBOUDT Karine³, JOURDAN Olivier², FEBVRE Guy², GOURBEYRE Christophe², GAYET Jean-Francois²

¹Kanazawa University, ²LaMP, ³LPCA

The POLARCAT (POLar study using Aircraft, Remote sensing, surface measurements and modelling of Climate, chemistry, Aerosols and Transport), is an international program endorsed as part of the 4th International Polar Year (IPY) in 2007 and 2008 (co-sponsored by ICSU/WMO), which aims to quantify the impact of trace gases, particulate aerosols and heavy metals transported to the Arctic and their contribution to pollutant deposition and climate change in the region. The contribution from the POLARCAT-France team (<http://www.polarcat.no/activities/polarcat-cnrs>) involved in-situ aircraft measurements to better quantify the impact of aerosol particle properties on the cloud characteristics in the Arctic during the spring 2008 campaign. The focus of this particular study is to conduct detailed characterization of individual cloud residual and interstitial aerosol particles collected using an airborne CVI (Counterflow Virtual Impactor), and provide insights into the cloud nucleating properties of the Arctic aerosols.

The ATR-42 research aircraft was stationed at Kiruna airport (67°50'N, 20°20'E, 460m a.m.s.l.) in the north of Sweden, from 30 March to 11 April 2008 during the POLARCAT-France spring measurement campaign. The aircraft made multiple level flights in the presence of cloud layers and pollution plumes in the low-mid troposphere (0.3-6 km). Tropospheric aerosol particles as well as residues from various clouds (ice, liquid or mixed phase) extracted by the CVI were analyzed later in the laboratory on individual particles basis under both Scanning and Transmission Electron Microscopes coupled to Energy Dispersive X-ray detectors (SEM- and TEM-EDX).

Submicron Biomass Burning (BB) particles (enriched in K, S and often internally mixed with soot) were characteristically found in polluted air-mass in the Arctic troposphere. Such BB particles were also extracted especially from liquid phase clouds but not as frequently from ice phase clouds. On the other hand, mineral dust, bare soot, flyash and marine (sea salt often enriched in K) particles dominated the submicron ice cloud residues.

The enrichment of marine particles in ice and mixed phase residues and abundance of BB particles as interstitial aerosols found in our study is surprisingly consistent with the results during CRYSTAL-FACE experiments (Cziczo et al., 2004). They also reported high abundance of sea salt found in the ice residue versus a low quantity found in the interstitial aerosol. BB related particles (those with mass spectral features owing to Sulfates, K+, Organics, and NO+), conversely, represents the vast majority of interstitial aerosol particles but with lower representation as ice residue. This similarity is striking considering the different analytical methods involved and geographical settings (i.e. cirrus clouds over Florida in 13km).

Reference:

Cziczo, D. J., Murphy, D. M., Hudson, P. K., & Thomson, D. S., Single particle measurements of the chemical composition of cirrus ice residue during CRYSTAL-FACE., *J. Geophys. Res.*, 109, D04201, 2004.

Acknowledgement:

POLARCAT-France campaigns was funded by the French research agencies ANR, CNES, CNRS-INSU (LEFE-CHAT), IPEV, EUFAR and CLIMSLIP-LEFE. Special thanks to SAFIRE for their support during the planning and execution of the French ATR-42 campaigns, and DT-INSU for their help with the instrument integration.

Mass spectrum analysis for aerosol particles with different hygroscopicity: Observation in the atmosphere of Nagoya

MOCHIDA, Michihiro^{1*}, SETOYUCHI, Yoshitaka¹

¹Graduate School of Environmental Studies, Nagoya University

The differences in the chemical composition from particle to particle in atmospheric aerosol are potentially very important to understand the roles of the particles in the atmosphere, e.g., the role as cloud condensation nuclei. Recent studies explored the relationship between the particle composition and the hygroscopicity based on single particle analysis (e.g., Zelenyuk et al., 2008; Herich et al., 2008), and demonstrated the capability of this method for the assessment of the aerosol mixing state. In this study, we performed single particle measurements for urban aerosols using an instrumental system that is a combination of a hygroscopicity tandem differential mobility analyzer (HTDMA) and a high resolution time-of-flight aerosol mass spectrometer (HR-ToF-AMS) equipped with a light scattering (LS) module.

Single particle mass spectrum analysis for urban aerosols were performed in Higashiyama Campus, Nagoya University, Nagoya, Japan from 8 to 15, November 2011. Sample aerosols that passed through a PM1 cyclone and diffusion dryers were introduced to the HTDMA. Particles with dry mobility diameters of 330 nm were selected in the first differential mobility analyzer (DMA) of the HTDMA, then the classified aerosol was humidified and introduced to the second DMA. The particles with different diameters under the humidified conditions were selected and introduced to the HR-ToF-AMS equipped with the LS module. The collected data were analyzed using the LS analysis software.

Both the increases in the LS and mass spectrum signals were observed at least for some of the recorded data, indicating a successful detection of single particles after the classification based on both size and hygroscopicity in the HTDMA. Preliminary analysis, although it is for a very small number of samples, shows that the mass spectra varied substantially depending on particles. Although more analyses, including the analysis about the particle detection efficiency, should be performed to adequately assess the performance of the observation using the system, the initial result suggests that this method is usefulness to understand the relationship between the chemical composition and the hygroscopicity of aerosol particles.

Analysis of chemical composition and size distribution of urban aerosol under three temperature conditions

SETOGUCHI, Yoshitaka^{1*}, Kaori Kawana¹, Shuhei Ogawa¹, Tomoki Nakayama², Yuka Ikeda², Yuki Sawada², Yutaka Matsumi², Michihiro Mochida¹

¹Graduate School of Environmental Studies, Nagoya University, ²Solar-Terrestrial Environment Laboratory, Nagoya University

Atmospheric aerosol components evaporate or condense as a result of the changes in air temperature. The volatility is an important property for the atmospheric lifetime of aerosol components because it could influence on the rate of chemical reactions and the removal by deposition. Recently, Huffman et al. (2009) reported atmospheric aerosol measurement using a high-resolution time-of-flight aerosol mass spectrometer (HR-ToF-AMS) coupled to a thermodenuder. Based on the measurements, they discussed the volatility of positive matrix factorization (PMF) components, i.e., hydrocarbon-like organic aerosol (HOA), semi-volatile oxygenated organic aerosol (SV-OOA), and low-volatility oxygenated organic aerosol (LV-OOA). Our knowledge on the volatility of PMF components including the relation to the size distribution is, however, still limited. In this study, we investigated the composition and size distribution of urban aerosols and assessed the differences under different temperature conditions.

The atmospheric observation was performed in Nagoya in August 2010. The chemical composition of aerosols was obtained by introducing them to HR-ToF-AMS after they passed through a PM1 cyclone, two diffusion dryers filled silica gel, and one of two heated pipes (100 and 300 degC) or a bypass tubing. We changed the temperature conditions that particles experienced to room temperature (RT), 100 degC, and 300 degC every 30 min. The data for the period from 16 to 25 August was analyzed.

In the first three days of the studied period, the concentrations of organics and inorganics were high. In the second three days, the concentration of nitrate was high in the morning on 21, whereas the concentrations of other components were low. In the last three days, the concentrations of organics and nitrate were low. Conversely, the concentrations of sulfate and ammonium were the highest in the morning of 23. The concentrations of chemical components at 100 and 300 degC were compared with those at RT. The mean concentrations of organics, nitrate, sulfate, and ammonium at 100 degC (or 300 degC) were, respectively, 73% (9%), 71% (18%), 94% (5%), and 91% (1%) of those at RT. While the concentrations of all these components decreased by the heating to 100 degC, the differences in the shape of the size distributions at different temperatures (RT and 100 degC) were not clear. We calculated the size distributions of PMF components at RT and 100 degC based on (1) a method using the intensities of three peaks in the mass spectra (m/z 43, 44, and 57) and (2) a method using the signals in 187 different m/z in each diameters. The sum of the size distributions of the PMF components calculated using these two methods agreed well with the size distributions of total organics. The centroid diameters (in the log scale) of the size distributions of the PMF components averaged for one day (from 06 to 06 LT) at RT and 100 degC were calculated. The averages (and ranges) for HOA, SV-OOA, and LV-OOA at RT were, respectively, 365 nm (325-403 nm), 362 nm (267-436 nm), and 502 nm (433-546 nm), and those at 100 degC were, respectively, 353 nm (314-454 nm), 336 nm (212-404 nm), and 497 nm (459-544 nm). Whereas the mean centroid diameter of LV-OOA was larger than the mean centroid diameters of HOA and SV-OOA, the mean centroid diameters of HOA and SV-OOA were similar regardless of the temperature conditions.

Keywords: aerosol mass spectrometer, positive matrix factorization

Changes of shape and composition of sea-salt aerosol particles in an urban atmosphere

ADACHI, Kouji^{1*}, IGARASHI, Yasuhito¹, BUSECK, Peter R.²

¹Meteorological Research Institute, ²Arizona State University

Sea salt is one of the most abundant natural aerosol particles and, thus, has important influences on local and global climate. Aerosol samples were collected in Los Angeles area during the CalNex (California Research at the Nexus of Air Quality and Climate Change) campaign in 2010. Their compositions and shapes were analyzed using transmission electron microscopes (TEMs). Sodium (Na), which characterizes sea salt aerosol (SSA) particles, was detected from 43% of analyzed particles with aerodynamic diameters between 50 and 300nm. Almost all those SSA particles also contain S. Although relatively fresh SSA particles contained Cl, many aged ones did not have Cl, suggesting that Cl was replaced with sulfate as they aged in the urban atmosphere. From TEM observations, SSA particles were classified either round- or sharp- edged ones. Round-edged SSA particles were more aged (>12 hour) and reacted with sulfate than sharp edged ones. Model calculations indicate that compositions and shapes of SSA particles, both of which change within several hours in urban atmosphere, affect their hygroscopicity and light scattering, respectively. These results indicate that the climate effects of SSA depend on their ages, and such effects need to be considered in climate modeling.

Keywords: Transmission electron microscope, sea salt aerosol particles, CalNex, atmospheric pollution, California, aerosol aging

Atmospheric aerosol particles collected above and below clouds along the pass of Mt. Fuji

UEDA, Sayako^{1*}, MIURA, Kazuhiko¹

¹Tokyo University of Science

Size and composition of atmospheric aerosol particles can be altered by in-cloud process with absorption/adsorption and drying of activated aerosol particles as cloud condensation nuclei. To elucidate differences of aerosol particles before and after in-cloud process, we made four sets of observations along the pass of Mt. Fuji, Japan (3776 m a.s.l.) during July and August 2011 using a portable optical particle counter and an aerosol sampler. Number concentrations of dried particles selected for cloud interstitial particles using a fog-cut impactor were measured to quantify tendencies of cloud activation condition in cloud. Aerosol samples for analysis of elemental composition were obtained above, in and below clouds, by using a cascade impactor. After shadowing by evaporation of Pt/Pd, individual particles on the samples were analyzed using a transmission electron microscopy (TEM) equipped with energy dispersive X-ray analyzer.

Clouds under up-wind conditions without rain were identified at three of the observations; the cloud altitudes were from 1700 m to 3300 m on 15th July, from 1300 m to 3300 m on 3rd August and from 2000 to 2400 m on 11th August. Aerosol number concentration above the clouds was one order lower than that below the clouds on 3rd August, but was equivalent with it on 15th July and 11th August. The backward air trajectories for 3rd August were also not similar altitudes of above and below the clouds. We compare the samples (for 15th July and 11th August) above and below cloud aerosols to identify the impacts of in-cloud process. Most of particles (0.5-2 μm diameter) were sea salt, containing Na with some S and Cl both for samples above and below the clouds. For Na-containing particles of 15th July, sample averages of atomic ratio of Cl/Na above and below the clouds were 0.00 and 0.30, respectively. In the atmosphere, NaCl in aerosol particles can be changed to Na_2SO_4 or NaNO_3 by substitution reaction. On 15th July, the ratio of S/Na above the clouds (0.20) was higher than that below the clouds (0.16), but lower than that of Na_2SO_4 (0.5), implying that Cl in the sea salt particles was replaced by SO_4 and other components in the clouds. For 11th August, the ratio of Cl/Na was 0.00 above and below the clouds, while the ratio of S/Na above the clouds (0.31) was higher than that below the clouds (0.17). This result suggests that SO_2 /sulfate components were absorbed or adsorbed onto sea salt particles after complete substitution of Cl.

Keywords: atmospheric aerosol particle, sea salt aerosol, in cloud process

Vertical distributions of aerosol constituents in the Antarctic troposphere during the ANTSYO-II: AGAMES campaign

HARA, Keiichiro^{1*}, HIRASAWA, Naohiko², YAMANOUCHI, Takashi², WADA Makoto², Andreas HERBER³

¹Fukuoka Univ., ²NIPR, ³AWI

During JARE48 (2006/2007), Japan-Germany cooperated airplane-borne aerosol measurement campaign (ANTSYO-II/AGAMES) was carried out around Neumayer, Kohlen and Syowa stations. This campaign aims to characterize aerosol properties in the summer Antarctic troposphere and understand spatial distributions and transport processes of aerosols. Here, we show the vertical distributions of aerosol constituents and their mixing states during the ANTSYO-II: AGAMES campaign.

Aerosol samples were taken using one-stage aerosol impactor (cut off diameter, ca. 0.2 micrometer) on board of "Polar-2" (Dornier 228, AWI). Aerosol measurements over Neumayer were made from 23 December 2006 till 31 December 2008 (including Kohlen flights on 28 ? 29 December), whereas the measurements around Syowa were carried out from 7 ? 24 January, 2007. Individual particles were observed and analyzed by TEM and SEM-EDX.

From the individual particle analysis, the following aerosol constituents were identified; (1) sulfate particles (sulfuric acid), (2) wholly Cl depleted sea-salt particles, (3) sea-salt particles containing Cl, (4) mineral particles, (5) CaSO₄ particles, (6) sulfate particles containing K, (7) sulfate particles containing Mg, and (8) phosphate particles. For quantitative comparison, relative abundance of each aerosol constituents was used in this study. Most of aerosol particles in all aerosol samples were sulfate particles without soot. Relative abundance of sulfate particles reached to >95 % in samples collected in the free troposphere. Although higher relative abundance of sea-salt particles and wholly modified sea-salt particles were obtained in the lower troposphere, high abundance of sea-salt particles was found in the middle free troposphere (3000 ? 6000 m). In contrast to higher abundance of wholly modified sea-salt particles in the boundary layer - lower free troposphere, abundance of sea-salt particles containing Cl was higher in the free troposphere. The vertical features of sea-salt particles were important information to understand transport processes from origin of sea-salt particles into Antarctic region. In addition, sulfate particles containing K were identified often in aerosol samples collected in the upper free troposphere. Although relative abundance of sulfate particles containing K was mainly <1%, abundance in aerosol samples collected in the upper free troposphere over Kohlen station reached to ca. 7 %. Because sulfate particles containing K can be released from combustion processes of fossil fuel and biomass, combustion-origin aerosol particles might be transported into the Antarctic regions via upper troposphere or lower stratosphere.

Keywords: aerosols, Antarctica, Troposphere, Spatial distributions

Development of online aerosol composition analyzers based on mass spectrometry

TAKEGAWA, Nobuyuki^{1*}, Takuma Miyakawa¹, Naoki Takeda², Masahiko Takei², Noritomo Hirayama²

¹RCAST, University of Tokyo, ²Fuji Electric, Co., Ltd.

Recent advances in on-line mass spectrometric analyzers have largely improved our understanding of sources and processes of ambient aerosols. Specifically, Aerodyne aerosol mass spectrometers (AMS) have widely been used by many investigators under various environments. The AMS utilizes an aerodynamic lens to generate particle beams and collects particles by impaction on a heated vaporizer. The evolved gas is analyzed by electron impact ionization (EI) mass spectrometry. While the AMS is useful for quantitative analysis of non-refractory materials, the particle collection efficiency is typically less than unity and varies depending on chemical composition. This is because liquid particles can be collected at high efficiency, but solid particles tend to bounce off the surface. We have developed a new analyzer for the online measurement of aerosol composition: a particle trap laser desorption mass spectrometer (PT-LDMS). The main components of the PT-LDMS include an inlet assembly (critical orifice, aerodynamic lens, etc.), a particle trap enclosed by a quartz cell, a quadrupole mass spectrometer (QMS) with electron impact ionization, and a carbon dioxide laser. The particle trap consists of custom-made mesh layers, the structure of which was newly designed to reduce the loss of particles due to bounce. The laser is used to vaporize aerosol compounds captured on the particle trap. The evolved gas confined within the quartz cell is analyzed using the QMS to quantify the chemical composition of the particles. The concept of the particle trap and laboratory evaluation of the instrument will be presented.

Keywords: Aerosol Composition, Particle trap, Laser desorption, Mass spectrometer, Online measurement

Measurement of fluorescence from a single-particle in the ambient air

TAKETANI, Fumikazu^{1*}, KANAYA, Yugo¹

¹JAMSTEC

It is well known that atmospheric aerosol which influences radiation budgets by scattering and absorbing is significant species. For aerosol measurement, optical techniques are adapted widely. Of the techniques, fluorescence is one of useful techniques for detecting organic compounds in the aerosol particles, especially biological one. In this study, we employed a single-particle fluorescence sensor for the detection of fluorescence particles, to test the possibility for the classification of organic aerosol in the ambient air.

The single-particle fluorescence sensor, WIBS4, is installed a continuous-wave 635nm diode laser for the detection of particles and the determination of particle size. A forward scattering quadrant photomultiplier tube (PMT) used for determination of particle size and shape. The instrument is also utilized two pulsed xenon UV sources emitting at different wavebands (280nm and 370nm) for the detection of fluorescence from an UV-excited particle.

We demonstrated ambient air measurement from April 20 to May 20, 2010 using WIBS4 instrument and PM2.5 mass concentration monitor at the Yokosuka campus of JAMSTEC. In the May 2-4, high mass concentrations of PM2.5 (>50 ug/m³) were observed. From the particle size and shape analysis by WIBS4 instrument in this period, it was suggested that the dust particles were measured. Also from fluorescence analysis, observed particles have fluorescence, suggesting that some dust particles contain the fluorescent compounds.

Keywords: fluorescence, single particle, atmospheric aerosol

Aerosol and cloud analyses using NIES lidar network observation data

NISHIZAWA, Tomoaki^{1*}, Sugimoto Nobuo¹, Matsui Ichiro¹, Shimizu Atsushi¹

¹National Institute for Environmental studies

We have established a ground-based lidar network (NIES lidar network) covering a wide area in East Asia since 2001 in order to monitor and understand the movements and the optical properties of Asian dust, air-pollution aerosols, and clouds. As part of the NIES lidar network observation, we have conducted shipborne lidar measurements using the research vessel MIRAI of JAMSTEC since 1999 in order to understand the optical properties of aerosols and clouds over ocean and provide vertical distribution data of aerosols and clouds for validation of numerical models and satellite-borne measurements. A compact two-wavelength (532 and 1064nm) backscatter (b) and one-wavelength (532nm) polarization (d) Mie-scattering lidar system (i.e., 2b+1d lidar system) with automatic measurement capability is used in the ground-based and shipborne observations. To better understand the optical properties of aerosols and clouds, we improved some lidars used in the ground-based lidar network observation by adding a channel measuring Raman scattering light from nitrogen gas. These improved lidars (Mie-Raman lidar system) can provide particle (i.e., aerosols and clouds) extinction data (a) at 532nm without assuming an extinction-to-backscatter ratio (i.e., 1a+2b+1d lidar system), unlike Mie-scattering lidar. We also constructed a new lidar system using High spectral resolution lidar (HSRL) technique; this lidar provides 1a (532nm), 2b (532 and 1064nm), and 1d (532nm) data like the Mie-Raman lidar. We installed the developed HSRL system on the vessel MIRAI and conducted the shipborne measurements over Indian ocean last year. To analyze the ground-based and shipborne 2b+1d lidar data, we developed algorithms to retrieve aerosol optical properties. The algorithms identify several main aerosol components in the atmosphere (e.g., dust, sea-salt, and air-pollution particles) and retrieve their extinction coefficients at each slab layer. These algorithms assume an external mixture of the aerosol components; mode radii, standard deviations and refractive indexes for each aerosol component are prescribed based on the literatures such as the Optical Properties of Aerosols and Clouds (OPAC) database; the optical properties for each aerosol component are computed from Mie theory on the assumption that their particles are spherical, except for dust. To consider the effect of nonsphericity, the dust optical properties are theoretically computed on the assumption that the particles are spheroidal. In these algorithm developments, we found that particle extinction data are useful to classify strongly light absorption particles. We are then developing an algorithm to identify black carbon particles as well as dust, sea-salt, and air-pollution particles with weak light absorption (e.g., sulfate and nitrate) using the ground-based and shipborne 1a+2b+1d lidar data. In the conference, we introduce the lidar systems used in the NIES lidar network observation and the observed data. We also present the outlines of the aerosol classification and retrieval algorithms and report the results of the application of the algorithms to the observed lidar data to demonstrate their abilities.

Keywords: aerosol, cloud, lidar, network observation

Impact of aerosols on tropospheric ozone photochemistry: Reduction of J values by dense aerosols at Rudong, China

KANAYA, Yugo^{1*}, Xiaole Pan¹, IRIE, Hitoshi¹, TAKETANI, Fumikazu¹, TAKASHIMA, Hisahiro¹, Zifa Wang²

¹RIGC/JAMSTEC, ²IAP/CAS

We conducted an intensive field campaign observing ozone and its precursors and chemical components/physical and optical parameters of aerosol particles at Rudong (32.26N, 121.37E), Jiangsu, China in May/June 2010 under international collaboration. The site is located at the west side of Yellow sea and is away from Shanghai by 100 km and from Rudong city center by 15 km. We measured spectral actinic flux in the UV/vis wavelength region by using a spectroradiometer. The actinic flux was then convoluted with the absorption cross section and the photodissociation quantum yield to obtain photolysis rates of O₃ (J(O₁D)) etc., important for studying photochemical activity such as in-situ photochemical production of O₃. J(O₁D) and J(NO₂) values around the noontime (SZA < 15 degrees) on cloudless days tend to significantly decrease with the aerosol optical depth (AOD, in a range of 0.17-1.26) determined by MAX-DOAS observations at 476 nm; the J(O₁D) and J(NO₂) values with AOD as high as 1.26 were only 58% and 74% of those with AOD as low as 0.17. The wide dynamic range in AOD there allowed us to characterize the decreases in J values. We used TUV ver. 4.6 radiative transfer model to calculate J values with variable AOD and single scattering albedo (SSA) values and they were compared with the observations (after correction to the values at total O₃ = 330 DU). The observed J(O₁D) and J(NO₂) values on May 24 and 25, when the AOD ranged from 0.19 and 0.35, were in agreement with the modeled values with SSA = 0.85 and 0.90, respectively. The observed J(O₁D) and J(NO₂) on June 23, when the AOD was in a higher range (1.09-1.26), showed good agreement with the model at SSA=0.95. The SSA ranges for the two periods were in good agreement with those independently estimated from the scattering and absorption coefficients determined by a nephelometer (at ambient RH conditions) and a MAAP (multi-angle absorption photometer) instrument, being 0.87 and 0.94, respectively. Such J value decreases caused by the aerosol are supposed to limit the present-day ozone production rates over China; future reduction in aerosol will increase J values and thereby the ozone production rate there.

Keywords: Aerosol, Ozone, Photolysis rate, aerosol optical density, single scattering albedo

Transboundary pollution in association with "cold surge" phenomena

WANG, Ping¹, Masaya Endo¹, Takao Suzuki¹, KITA, Kazuyuki^{1*}, OGINO, Shin-Ya², Seiichirou Yonemura³, Boossarasiri Thana⁴

¹Faculty of Science, Ibaraki University, ²JAMSTEC, ³NIAES, ⁴Chularonkorn University

Tropospheric ozone plays crucial roles on the environment in the lower troposphere. In southeast Asia, active biomass burning and increasing human activities may increase the tropospheric ozone. In addition, transboundary transport of polluted air from China and/or India may affect the tropospheric ozone in this region.

We have continuously monitored surface ozone and carbon monoxide concentration at Phimai, mid-east Thailand since 2007. Variations of the ozone and CO concentration are discussed in terms of the backward trajectories from Phimai. While they were very low in the wet season between late May and September, when monsoon brings air masses over Indian Ocean, they significantly increased during the dry season. In the early dry season, between late October and December, they repeatedly increased and decreased. A meteorological analysis indicates that this semi-oscillating phenomenon occurred in association with the "cold-surge" phenomenon, which transports relatively cold and high-pressure air from the inland of Asian continent, leading to transboundary transport of heavily-polluted air masses over south China. In the late dry season, a westerly wind brought polluted air in the southern urban areas such as Bangkok. In addition, increasing diurnal variation of CO implies that biomass burning in the surrounding area affected the CO and ozone level.

Keywords: tropospheric ozone, southeast Asia, transboundary pollution, cold surge

Regional differences in the photochemical reaction paths of NO_X estimated from the D^{17}O tracer of nitrate

OHYAMA, Takuya^{1*}, TSUNOGAI, Urumu¹, KOMATSU, Daisuke¹, NAKAGAWA, Fumiko¹, Izumi Noguchi², Takashi Yamaguchi², Keiichi Sato³, Tsuyoshi Ohizumi³, TSUBOI, Kazuhiro⁴, Mizuka Kido⁵

¹Faculty of Sci., Hokkaido University, ²Hokkaido Res. Org., Inst. Environ. Sci., ³Asia Center for Air Pollution Res., ⁴Meteorological Res. Inst., ⁵Toyama Pref. Environ. Sci. Res.

Anthropogenic activities emitted large quantities of NO_X to the atmosphere. NO_X are oxidized to nitrate via photochemical reactions with O_3 and OH radical. The photochemically produced nitrate finally deposited on to surface environments as dry and wet depositions during polluted air-mass transport. Increasing anthropogenic activities could increase the deposition flux. Besides, they could also change the photochemical reaction paths. However, it is difficult to determine the major photochemical path through the observation only on the concentration of either NO_X in atmosphere or nitrate in wet deposition.

The triple oxygen isotopic composition ($\text{D}^{17}\text{O} = \text{d}^{17}\text{O} - 0.52 * \text{d}^{18}\text{O}$) of nitrate can be a useful tracer to quantify the contribution of O_3 within the photochemical paths. The photochemically produced nitrate via O_3 having large ^{17}O anomaly shows large D^{17}O value, whereas that via OH radical, by contrast, shows small D^{17}O value. Thus, we could clarify the major photochemical oxidation path of NO_X using D^{17}O values of depositional nitrate.

We have collected wet deposition (precipitation) samples extensively in Japan (Figure 1). Except for the site in sub-tropical region (Minamitorishima), the D^{17}O values of nitrate showed distinct seasonal variations. In summer, the reaction between NO_X and OH is the dominant photochemical oxidation path for the production of nitrate. In contrast, the reaction of NO_X with O_3 becomes relatively important in winter. In addition, we found that the annual average D^{17}O values at Sado-Seki and Kosugi were larger than that at Rishiri located at high latitude (Figure 1). Generally, as the contributions of O_3 increase with latitude, the annual average D^{17}O values become larger in higher latitude. The inverse latitudinal distributions of D^{17}O value can be explained by regional differences in the photochemical reaction paths of NO_X .

Keywords: triple oxygen isotope, photochemical reaction paths, nitrate

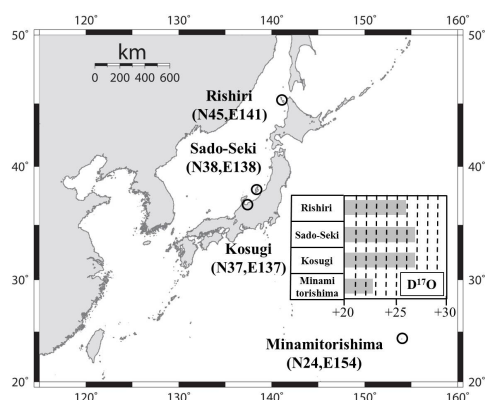


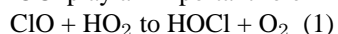
Figure 1 Sampling locations and annual average D^{17}O values

Estimation of the reaction rate constant of $\text{ClO} + \text{HO}_2$ to $\text{HOCl} + \text{O}_2$ by SMILES observation

KURIBAYASHI, Kouta^{1*}, SAGAWA, Hideo², SATO, Tomohiro¹, KASAI, YASUKO²

¹Tokyo institute of Technology, ²NICT

HOCl play an important role in the ozone chemistry to link the odd ClO_x and the odd HO_x with the reaction,



This is the only one reaction to produce HOCl in the middle atmosphere in the gas phase. This reaction is a key in the middle stratospheric ozone loss for the partitioning of the Cl atomic radical.

There are several laboratory studies to determine the reaction rate constant of (1). But these reaction rate constants have large discrepancies with large uncertainties as $k_{\text{HOCl}} = 3.3 \times 10^{-11} \exp(-850/T) + 4.5 \times 10^{-12} (T/300)^{-3.7}$ (Stimpfle et al, 1979) or $k_{\text{HOCl}} = (1.75 \pm 0.52) \times 10^{-12} \exp[(368 \pm 78)/T]$ (Hickson et al, 2007). Main reason for its uncertainty is that the chemical reaction of (1) is the reaction of ClO radical and HO₂ radical. Therefore, in laboratory experiment for the calculation of this reaction rate constant, the generations of two radical is too difficult, and it is also difficult to extract only this reaction purely.

We have estimated the reaction rate constant of (1) from the atmospheric observation directly in the upper stratosphere/ lower mesosphere (US/LM) region by using a new super-sensitive remote sensing technology named Superconducting SubMillimeter-wave Limb Emission Sounder (SMILES) on the International Space Station (ISS)

We had estimate the reaction rate constant of (1) with the procedure as below.

1) We discovered that the time period when the reaction of (1) was purely happened is from one hour after sunset to one hour before sunrise.

2) From the time variations of ClO and HO₂ of this time period, we calculated the reaction rate constant of (1). The estimated reaction rate constant is $8.9 \times 10^{-12} [\text{cm}^3 \text{ molecule}^{-1} \text{ s}^{-1}]$ (20S-40S, 0.54hPa, 254.5K)

3) From this reaction rate constant and the time variations of ClO and HO₂, we calculated the time variations of HOCl.

4) We checked the comparison between these calculated values and observed values. Our calculated values was in good agreement with the observed values.

5) We checked the comparison between our estimated reaction rate constants and the previous reaction rate constants. Our estimated reaction rate constant, $k_{\text{HOCl}} = 8.9 \times 10^{-12}$ (20S-40S, 0.54hPa, 254.5K), was between the reaction rate constant, $k_{\text{HOCl}} = 7.43 \times 10^{-12}$ (Hickson et al), and the reaction rate constant, $k_{\text{HOCl}} = 9.44 \times 10^{-12}$ (Stimpfle et al).

Keywords: SMILES, HOCl

Seasonal variations of greenhouse gases observed in the free-troposphere using a C-130H cargo aircraft

NIWA, Yosuke^{1*}, TSUBOI, Kazuhiro¹, MATSUEDA, Hidekazu¹, SAWA, Yousuke¹, Masamichi Nakamura², Daisuke Kuboike², Kazuyuki Saito², Hidehiro Ohmori², Shohei Iwatsubo², Hidehiro Nishi², Yoshikazu Hanamiya², Kentaro Tsuji², Yusuke Baba², MACHIDA, Toshinobu³

¹Meteorological Research Institute, ²Japan Meteorological Agency, ³National Institute for Environmental Studies

Atmospheric measurements of greenhouse gases (GHGs) are conducted mostly at ground-based stations. Therefore, spatial and temporal variations of GHGs in the free-troposphere are not fully understood. Since February 2011, Japan Meteorological Agency has operated air flask sampling measurements of carbon dioxide (CO₂), carbon monoxide (CO), methane (CH₄), and nitrous oxide (N₂O) using a C-130H cargo aircraft in cooperation with the Ministry of Defense. The aircraft flies from Kanagawa to Minamitori-shima over the western North Pacific once a month, collecting about 20 and 4 air samples during cruising and descending sections respectively. The cruising altitude is about 6 km, where all the measurements represent free-tropospheric concentrations. It was well captured that the seasonal cycle of the observed CO₂ concentration shows a maximum during April-May and a minimum in September. However, detailed seasonal patterns are apparently different in vertical from the surface to 6 km altitude. Especially, the steep vertical gradients of CO₂ are prominent during winter and spring seasons. It was also found that high-concentration events of CO appeared in the mid free-troposphere during the spring season. These characteristic features strongly suggest a large impact of Asian continental outflow on the greenhouse gases distributions in the free-troposphere. By comparing three-dimensional simulation results with the aircraft measurements, the East Asian emissions and structures of the Asian continental outflow are examined.

Keywords: greenhouse gases, aircraft observation, free-troposphere

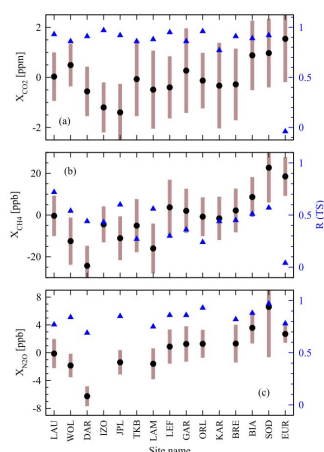
Latitude-time variations of atmospheric column-average dry air mole fractions of CO₂, CH₄ and N₂O

SAITO, Ryu^{1*}, PATRA, Prabir¹, ISHIJIMA, Kentaro¹

¹JAMSTEC

We present a comparison of an atmospheric general circulation model (AGCM)-based chemistry-transport model (ACTM) simulation with total column measurements of CO₂, CH₄ and N₂O from the Total Carbon Column Observing Network (TCCON). The model is able to capture observed trends, seasonal cycles and interhemispheric gradients at most sampled locations for all three species. The model-observation agreements are best for CO₂, because the simulation uses fossil fuel inventories and an inverse model estimate of non-fossil fuel fluxes. The ACTM captures much of the observed seasonal variability in CO₂ and N₂O total columns (~81% variance, $R > 0.9$ between ACTM and TCCON for 19 out of 22 cases). These results suggest that the transport processes in troposphere and stratosphere are well represented in ACTM. Thus the poor correlation between simulated and observed CH₄ total columns, particularly at tropical and extratropical sites, have been attributed to the uncertainties in surface emissions and loss by hydroxyl radicals. While the upward-looking total column measurements of CO₂ contains surface flux signals at various spatial and temporal scales, the N₂O measurements are strongly affected by the concentration variations in the upper troposphere and stratosphere.

Keywords: CO₂, CH₄, N₂O, Atmospheric Transport Model, TCCON



Observations of atmospheric radiocarbon in carbon dioxide at Hateruma Island

TERAO, Yukio^{1*}, MUKAI Hitoshi¹, TOHJIMA, Yasunori¹, MAKSYUTOV, Shamil¹

¹Center for Global Environmental Research, National Institute for Environmental Studies

We have been conducted monthly air samplings for measurements of atmospheric radiocarbon in carbon dioxide ($^{14}\text{CO}_2$) at Hateruma Island (HAT, 24.05°N, 123.80°E, 47 m a.s.l.), Japan since 2004. We collected whole air samples using 2.5L glass flasks pressurized to 2.3 atm, and 5L air was used for radiocarbon analysis. The values of $\Delta^{14}\text{C}$ were measured using Compact Accelerator Mass Spectrometry (CAMS, NEC 1.5SDH). Uncertainty in $\Delta^{14}\text{C}$ measured by CAMS is less than 2 per mil, which is based on the number of ^{14}C counts and the scatter of $^{14}\text{C}/^{12}\text{C}$ ratios during measurements. The reproducibility of CAMS measurements is ± 1.4 per mil (standard deviation of $\Delta^{14}\text{C}$ values in a reference air cylinder). The $\Delta^{14}\text{C}$ values of background maritime air observed at HAT clearly show the seasonal cycle (minimum in March and October and maximum in August) with amplitude of 10 per mil. The simulation using atmospheric transport model (NIES TM) indicates that fossil fuel CO_2 causes seasonal cycle of $\Delta^{14}\text{C}$.

In HAT we can measure polluted continental air from the East Asia in winter. To capture the high CO_2 events of Asian outflow, we installed remote-controlled autosampling system at HAT in 2010. For example, between March 7 and 11, 2010, we observed two events of CO_2 enhancement. The $\Delta^{14}\text{C}$ values in the high CO_2 samples were significantly lower than the background level. The $\Delta^{14}\text{C}$ observations indicate that fossil fuel CO_2 contributes 73-83% of CO_2 enhancement in the first event and 47-72% in the second event. The simulation suggests that biospheric emissions cause the other part of CO_2 enhances. The keeling plot of $\Delta^{14}\text{C}$ shows the difference between two events clearly rather than that of $\delta^{13}\text{C}$, implying advantage of high precision $\Delta^{14}\text{C}$ measurements for CO_2 source appointment.

Keywords: carbon cycle, carbon isotope measurements, Accelerator Mass Spectrometry, Asian outflow, source appointment, atmospheric transport

Interannual variations of the oceanic and the land biospheric CO₂ uptake estimated based on atmospheric O₂/N₂ ratio

ISHIDOYA, Shigeyuki^{1*}, MORIMOTO, Shinji², AOKI, Shuji³, Shoichi Taguchi¹, GOTO, Daisuke³, NAKAZAWA, Takakiyo³

¹AIST, ²National Institute of Polar Research, ³Tohoku University

To investigate interannual variations of the oceanic and the terrestrial biospheric CO₂ uptake within 10 years based on the observation of Atmospheric Potential Oxygen (APO = O₂ + 1.1 × CO₂), the APO observed at Ny-Alesund, the Arctic and Syowa, Antarctica for the period 2001-2009 are analyzed. The interannual variations of air-sea O₂ flux due to a change of the ocean heat content is simulated using an atmospheric transport model with a global fields of the upper ocean heat content and a coefficient of air-sea O₂ flux / heat flux. The observed and the simulated increase rates of APO are in phase, and the interannual variation of the estimated oceanic CO₂ uptake using the corrected increase rate of APO for the variation of air-sea O₂ flux is lower than +0.6 GtC yr⁻¹. This variation is comparable to those reported by previous studies using an atmospheric inversion or ocean biogeochemical model. It is also suggested that the land biosphere emits CO₂ to the atmosphere around El Nino event in 2002-2003, as well as the oceanic CO₂ uptake is relatively smaller around La Nina event than that around El Nino event. The average oceanic CO₂ uptake is estimated to be 2.9±0.8 GtC yr⁻¹ for the period 2001-2009, and the terrestrial biospheric CO₂ uptake for the period 2004-2009, i.e. excluding its drop-off around 2002-2003, is estimated to be 1.7±0.9 GtC yr⁻¹.

Keywords: Atmospheric O₂/N₂ ratio, Atmospheric Potential Oxygen, Interannual variation of anthropogenic CO₂ budget, Ocean heat content, Air-sea O₂ flux

Comparison of CO₂ vertical profiles measured by balloon-borne instrument measurements with aircraft measurements

OHUCHI, Mai^{1*}, MATSUMI, Yutaka¹, NAKAYAMA, Tomoki¹, MACHIDA, Toshinobu², MATSUEDA, Hidekazu³, SAWA, Yousuke³, Tomoaki Tanaka⁴, Isamu Morino², Osamu Uchino²

¹Nagoya University Solar-Terrestrial Environment Laboratory, ²National Institute for Environmental Studies, ³Geochemical Research Department, Meteorological Research Institute, ⁴Japan Aerospace Exploration Agency

The atmospheric CO₂ concentration has drastically increased since the Industrial Revolution due to the mass consumption of fossil fuels and natural gas by human activities. CO₂ is considered to be a major factor of global warming; therefore it is very important to measure CO₂ correctly. Current CO₂ monitoring sites are limited and there are not many CO₂ vertical profile measurements.

We are developing balloon-borne instruments which can measure the vertical distribution of CO₂ in any place in the world under any kind of weather conditions. The objective is to contribute to raise the precision of climate change prediction by utilizing the balloon-borne instruments all over the world like ozone sonde instruments.

We will present comparisons of balloon-borne instrument results and aircraft measurement results in order to validate the balloon-borne instruments precision.

We used two types of aircraft data for the comparison analyses, one is CONTRAIL(Comprehensive Observation Network for Trace gases by AirLiner) data of passenger aircraft CO₂ measurements and the other is the data obtained by aircraft measurements performed by JAXA and NIES for validation of the GOSAT satellite.

Firstly, we compared the data obtained on 7 January 2011 using the balloon-borne instruments at three sites (Isezaki, Ichihara, and Shirako) with the CONTRAIL data. Secondly, we compared two data obtained on 31 January and on 3 February 2011 using the balloon-borne instruments at Moriya with the JAXA/NIES aircraft measurements at Tsukuba.

Keywords: carbon dioxide, balloon-borne measurement, aircraft